International Journal of Fracture **88:** 41–59, 1997.

A general boundary element analysis of 2-D linear elastic fracture mechanics

ERNIAN PAN
Department of Mechanical Engineering, University of Colorado at Boulder, CO 80309

Received 12 November 1996; accepted in revised form 8 August 1997

Abstract. This paper presents a boundary element method (BEM) analysis of linear elastic fracture mechanics in two-dimensional solids. The most outstanding feature of this new analysis is that it is a single-domain method, and yet it is very accurate, efficient and versatile: Material properties in the medium can be anisotropic as well as isotropic. Problem domain can be finite, infinite or semi-infinite. Cracks can be of multiple, branched, internal or edged type with a straight or curved shape. Loading can be of in-plane or anti-plane, and can be applied along the no-crack boundary or crack surface. Furthermore, the body-force case can also be analyzed.

The present BEM analysis is an extension of the work by Pan and Amadei (1996a) and is such that the displacement and traction integral equations are collocated, respectively, on the no-crack boundary and on one side of the crack surface. Since in this formulation the displacement and/or traction are used as unknowns on the no-crack boundary and the relative crack displacement (i.e. displacement discontinuity) as unknown on the crack surface, it possesses the advantages of both the traditional displacement BEM and the displacement discontinuity method (DDM) and yet gets rid of the disadvantages associated with these methods when modeling fracture mechanics problems. Numerical examples of calculation of stress intensity factors (SIFs) for various benchmark problems were conducted and excellent agreement with previously published results was obtained.

Key words: Single-domain BEM, stress intensity factor, fracture mechanics, anisotropic elasticity

1. Introduction

The boundary element method (BEM) has proven to be a powerful numerical technique which has certain advantages over the domain-based method such as the finite element method. The most important feature of the BEM is, as is well-known, that it only requires discretization of the boundary rather than the domain.

Stress intensity factors (SIFs) are important in the analysis of cracked materials. They are directly related to the fracture propagation and fatigue crack growth criteria. The singularity of stresses near a crack-tip and the geometry identity of the two surfaces of a crack have challenged all the previous numerical modeling methods, even the BEM. For handling of these difficulties, several methods within the scope of the BEM have been suggested previously (Par and Amadei, 1996a; Aliabadi, 1997). The first one is the Green's function method (Snyder and Cruse, 1975), which has the advantage of avoiding crack surface modeling and gives excellent accuracy. It is however, restricted to fracture problems involving very simple crack geometries for which analytical Green's functions can be obtained. The second one is the multi-domain technique (Blandford et al., 1981, Sollero et al., 1994, Sollero and Aliabadi, 1995). The advantage of this approach is its ability to model cracks with any geometric shape. The disadvantage is an artificial subdivision of the original domain into several sub-domains, thus resulting in a large system of equations. The third approach is the displacement discontinuity method (DDM) (Crouch and Starfield, 1983). Instead of using the Green's displacements and stresses from point forces, the DDM uses Green's functions corresponding

to point dislocations (i.e., displacement discontinuities). This method is quite suitable for crack problems in infinite domains where there is no no-crack boundary. However, it alone may not be efficient for finite domain problems, since the kernel functions in DDM invovle singularities with order higher than those in the traditional displacement BEM.

In recent years, several single-domain BEMs have been proposed for the study of cracked media (Hong and Chen, 1988; Gray et al., 1990; Portela et al., 1992; Sollero and Aliabadi, 1995a, 1995b; Sur and Altiero, 1988; Liu et al., 1990; Liu and Altiero, 1991, 1992, Ammons and Vable, 1996; Chang and Mear, 1995). These single-domain BEMs involve two sets of boundary integral equations (one is the displacement integral equation, and another is either the traction or the stress-function integral equation), and are, in general, superior to the aforementioned BEM's.

One of the single-domain BEMs is the so-called Dual Boundary Element Method (DBEM) (Portela et al., 1992; Aliabadi, 1997) where the displacement integral equation is collocated on the no-crack boundary and on one side of the crack surface while the traction integral equation is collocated on the other side of the crack surface. The hypersingularity involved in the traction integral equation is evaluated analytically by assuming a piece-wise flat crack path. Extension of this DBEM formulation to the plane anisotropic crack problem was reported in (Sollero and Aliabadi, 1995a, 1995b).

In the DBEM formulation, the displacement on each side of the crack surface is collocated as unknown. Thus, the resulting algebraic equations are doubled along the crack surface, which may be unnecessary for the SIF calculation. Therefore, an ideal single-domain BEM formulation would be the one which requires discretization on one side of the crack suface only. Such single-domain BEM formulation can be achieved by applying the displacement integral equation to the no-crack boundary only, and the traction or the stress- function integral equation on one side of the crack surface only. Since only one side of the crack surface is collocated, one needs to choose either the relative crack displacement (RCD) (Sur and Altiero, 1988; Ammons and Vable, 1996) or the tangential derivative of the RCD (Chang and Mear, 1995) as unknown. Although using the tangential derivative of the RCD can reduce the singularity order in the traction integral equation, the tangential derivative of the RCD is singular at crack-tips and kinks (Sur and Altiero, 1988). Therefore, difficulty may arise when modeling kinked and/or branched cracks with this approach (Sur and Altiero, 1988; Chang and Mear, 1995).

In a recent paper, a new single-domain BEM formulation was proposed by Pan and Amadei (1996a) for the calculation of the SIFs in cracked 2-D anisotropic materials. The new formulation is similar to the BEM formulations of Liu et al. (1990); Ammons and Vable (1996) for the isotropic medium in which the RCD is selected as unknown on the crack surface. As in Liu et al. (1990), the displacement integral equation is collocated on the no-crack boundary; But on one side of the crack surface, the traction integral equation, instead of the stress function integral equation (Liu et al., 1990), is applied (Pan and Amadei, 1996a). While the Cauchy integration in the displacement integral equation was evaluated analytically by the rigid-body motion method, the hypersingularity in the traction integral equation was handled by an accurate numerical integration similar to the Gauss quadrature (Tsamasphyros and Dimou, 1990; Pan and Amadei, 1996a). The most outstanding feature of this new formulation is that it can be applied to the general fracture mechanics analysis in anisotropic media while keeping the single-domain merit.

This paper is a result of the author's continuing effort on the BEM modeling of fracture mechancis problems. It is based on the work by Pan and Amadei (1996a), but is extended in

several aspects to make the formulation unified and yet versatile. In the previous work by Pan and Amadei (1996a), the J-integral was used to calculate the SIFs. This method, though very accurate, has difficulty for handling the body-force, pressurized crack, and curved crack cases. In this paper, we proposed the extrapolation method of the RCD, combined with a new set of crack-tip shape functions. The important feature of our extrapolation method is that it is very flexible and yet very accurate. For the second extension, the complete Green's functions in a generally anisotropic half-plane have also been incorporated into our new BEM formulation so that the half-plane, finite and infinite domains can all be considered in a unified form. As a final extension, all the mode III-related equations have been derived and included in the current formulation, which can be used to analyze anti-plane problems.

Numerical examples involving different loading and geometry conditions were selected for the calculation of the SIFs. For all cases, it was found that the SIFs by the current single-domain BEM formulation were in excellent agreement with the previously published analytical or numerical results.

2. BEM formulation for 2-D cracked anisotropic media

For a linear elastic medium, we express, by superposition, the total displacements, stresses, and tractions as follows

$$u_i^t = u_i^h + u_i^p; \qquad \sigma_{ij}^t = \sigma_{ij}^h + \sigma_{ij}^p; \qquad T_i^t = T_i^h + T_i^p, \tag{1}$$

Following the procedure by Pan and Amadei (1996a,b), one can show that the total internal displacement solution can be expressed by the following integral

$$\begin{aligned} &u_i^t(\mathbf{X}_p) + \int_S T_{ij}^*(\mathbf{X}_p, \mathbf{X}_S) u_j^t(\mathbf{X}_S)\, \mathrm{d}S(\mathbf{X}_S) + \int_\Gamma T_{ij}^*(\mathbf{X}_p, \mathbf{X}_{\Gamma+})[u_j^t(\mathbf{X}_{\Gamma+}) - u_j^t(\mathbf{X}_{\Gamma-})]\, \mathrm{d}\Gamma(\mathbf{X}_{\Gamma+}) \\ &= \int_S U_{ij}^*(\mathbf{X}_p, \mathbf{X}_S) T_j^t(\mathbf{X}_S)\, \mathrm{d}S(\mathbf{X}_S) + \int_S T_{ij}^*(\mathbf{X}_p, \mathbf{X}_S)(u_j^p(\mathbf{X}_S) - u_i^p(\mathbf{X}_p))\, \mathrm{d}S(\mathbf{X}_S) \\ &\quad - \int_S U_{ij}^*(\mathbf{X}_p, \mathbf{X}_S) T_j^p(\mathbf{X}_S)\, \mathrm{d}S(\mathbf{X}_S), \end{aligned} \tag{2}$$

where $\mathrm{d}S$ and $\mathrm{d}\Gamma$ are the line elements on the no-crack boundary and crack surface, respectively, with the corresponding points being distinguished by subscript s and Γ (Figure 1). A point on the positive (or negative) side of the crack is denoted by $\mathbf{X}_{\Gamma+}$ (or $\mathbf{X}_{\Gamma-}$); U_{ij}^* and T_{ij}^* are the Green's displacements and tractions which will be derived in the next section. We add that, in deriving (2), we have assumed that the tractions on the two faces of a crack are equal and opposite.

Let $\mathbf{X}_p$ approach a point $\mathbf{Y}_S$ on the no-crack boundary, one arrives at the following boundary integral equation

$$\begin{aligned} &b_{ij} u_j^t(\mathbf{Y}_S) + \oint_S T_{ij}^*(\mathbf{Y}_S, \mathbf{X}_S) u_j^t(\mathbf{X}_S)\, \mathrm{d}S(\mathbf{X}_S) \\ &\quad + \int_\Gamma T_{ij}^*(\mathbf{Y}_S, \mathbf{X}_{\Gamma+})[u_j^t(\mathbf{X}_{\Gamma+}) - u_j^t(\mathbf{X}_{\Gamma-})]\, \mathrm{d}\Gamma(\mathbf{X}_{\Gamma+}) \\ &= \int_S U_{ij}^*(\mathbf{Y}_S, \mathbf{X}_S) T_j^t(\mathbf{X}_S)\, \mathrm{d}S(\mathbf{X}_S) + \end{aligned}$$

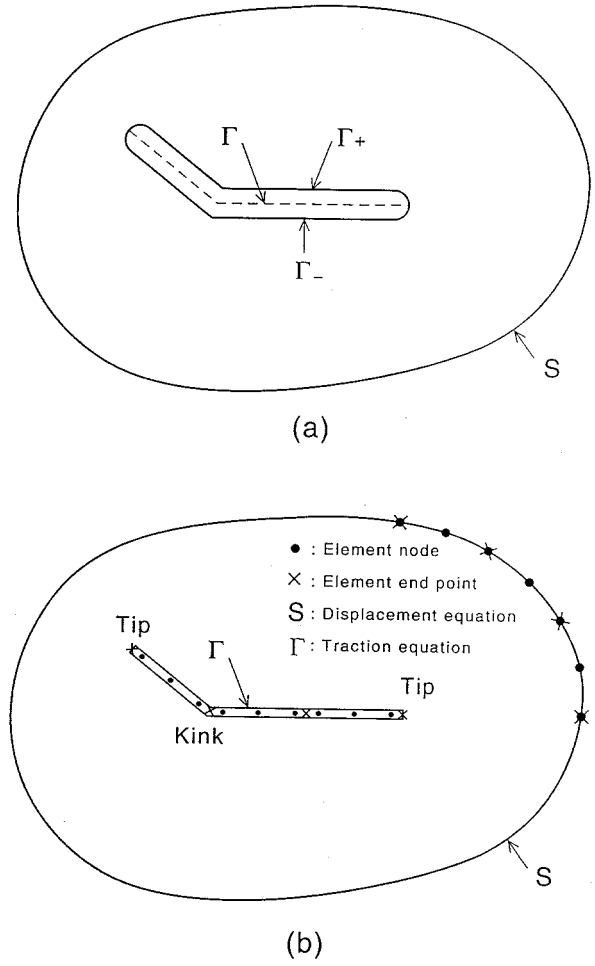

Figure 1. Geometry of a cracked 2-D anisotropic domain in (a), and its modeling with quadratic boundary elements in (b).

$$+\int_S T_{ij}^*(\mathbf{Y}_S,\mathbf{X}_S)(u_j^p(\mathbf{X}_S)-u_i^p(\mathbf{Y}_S))\,\mathrm{d}S(\mathbf{X}_S)$$

$$-\int_S U_{ij}^*(\mathbf{Y}_S,\mathbf{X}_S)T_j^p(\mathbf{X}_S)\,\mathrm{d}S(\mathbf{X}_S), \tag{3}$$

where b_{ij} are coefficients that depend only upon the local geometry of the no-crack boundary at $\mathbf{Y}_S$

It is observed that all the terms on the right-hand side of (3) have only weak singularities, thus, are integrable. Although the second term on the left-hand side of (3) has a strong singularity, it can be treated by the rigid-body motion method. At the same time, the calculation of b_{ij} can also be avoided.

It is well-known, however, that for a cracked domain, (3) does not have a unique solution (Aliabadi, 1997). For this situation, the traction integral equation (Pan and Amadei, 1996a) can be employed. Assume that Y_Γ is a smooth point on the crack surface, the traction integral

equation can be derived as

$$
\begin{aligned}
&0.5[T_l^t(\mathbf{Y}_{\Gamma+}) - T_l^t(\mathbf{Y}_{\Gamma-})] + n_m(\mathbf{Y}_{\Gamma+}) \int_S c_{lmik} T^*_{ij,k}(\mathbf{Y}_{\Gamma+}, \mathbf{X}_S) u_j^t(\mathbf{X}_S)\, \mathrm{d}S(\mathbf{X}_S) \\
&\quad + n_m(\mathbf{Y}_{\Gamma+}) \text{⨍}_t\, c_{lmik} T^*_{ij,k}(\mathbf{Y}_{\Gamma+}, \mathbf{X}_{\Gamma+})[u_j^t(\mathbf{X}_{\Gamma+}) - u_j^t(\mathbf{X}_{\Gamma-})]\, \mathrm{d}\Gamma(\mathbf{X}_{\Gamma+}) \\
&= 0.5[T_l^p(\mathbf{Y}_{\Gamma+}) - T_l^p(\mathbf{Y}_{\Gamma-})] + n_m(\mathbf{Y}_{\Gamma+}) \int_S c_{lmik} U^*_{ij,k}(\mathbf{Y}_{\Gamma+}, \mathbf{X}_S) T_j^t(\mathbf{X}_S)\, \mathrm{d}S(\mathbf{X}_S) \\
&\quad + n_m(\mathbf{Y}_{\Gamma+}) \int_S c_{lmik} T^*_{ij,k}(\mathbf{Y}_{\Gamma+}, \mathbf{X}_S) u_j^p(\mathbf{X}_S)\, \mathrm{d}S(\mathbf{X}_S) \\
&\quad - n_m(\mathbf{Y}_{\Gamma+}) \int_S c_{lmik} U^*_{ij,k}(\mathbf{Y}_{\Gamma+}, \mathbf{X}_S) T_j^p(\mathbf{X}_S)\, \mathrm{d}S(\mathbf{X}_S), \qquad (4)
\end{aligned}
$$

where n_m is the outward normal at the crack surface $\mathbf{Y}_{\Gamma+}$ and c_{lmik} is a 4th order stiffness tensor.

Equations (3) and (4) form a new pair of boundary integral equations, and they are similar to the single-domain BEMs of Liu et al. (1990) and Ammons and Vable (1996) for the isotropic medium. In this new formulation, the displacement integral equation is collocated on the no-crack boundary only; But on one side of the crack surface only, it is the traction integral equation, instead of the stress-function integral equation, which is applied. Therefore, as in Liu et al. (1990) and Ammons and Vable (1996), no double elements and nodes are required along the crack surface. Furthermore, this formulation can be applied to generally anisotropic media with the Cauchy type integral being evaluated exactly by the rigid-body motion method. It is also worthy to mention that the effect of the body force and/or far-field stresses have been included by superposing the corresponding particular solution, which makes the problem very similar to the one associated with the homogeneous governing equations. The only difference is that for the body force and/or far-field stress cases, two extra integral terms related to the particular solution need to be added to the homogeneous integral equations. The advantage of using (3) and (4) is that for the far-field stress case, the artificial truncation of the infinite domain (Lee, 1995) or transferring of the far-field stress onto the problem boundary (Telles and Brebbia, 1981; Dumir and Mehta, 1987) can be avoided. While the former method increases the size of the problem and also introduces errors because of the truncation of the region, the latter may not be suitable for cases where the boundary has a complex shape.

For problems containing crack surfaces only, i.e., cracks in an infinite or a half plane, only (4) is required with the no-crack boundary integral terms being omitted.

The boundary integral equations (3) and (4) can be discretized and solved numerically for the unknown boundary displacements (or displacement discontinuities on the crack surface) and tractions. The hypersingular integral term in (4) is handled by an accurate and efficient Gauss quadrature formulae (Tsamasphyros and Dimou, 1990; Pan and Amadei, 1996), which is similar to the traditional weighted Gauss quadrature but with a different weight.

In order to capture the square-root characteristics of the RCD near the crack-tip, we construct the following crack-tip element with its tip at $s = -1$

$$
\Delta u_i = \sum_{k=1}^{3} \phi_k \Delta u_i^k, \qquad (5)
$$

where the subscript $i(=1,2,3)$ denotes the components of the RCD, and the superscript $k(=1,2,3)$ denotes the RCD at nodes $s=-\frac{2}{3}, 0, \frac{2}{3}$, respectively. The shape functions ϕ_k are

$$\begin{aligned}
\phi_1 &= \frac{3\sqrt{3}}{8}\sqrt{s+1}[5-8(s+1)+3(s+1)^2],\\
\phi_2 &= \frac{1}{4}\sqrt{s+1}[-5+18(s+1)-9(s+1)^2],\\
\phi_3 &= \frac{3\sqrt{3}}{8\sqrt{5}}\sqrt{s+1}[1-4(s+1)+3(s+1)^2].
\end{aligned} \tag{6}$$

Our numerical tests have shown that solutions of (3) and (4) based on these new shape functions are more accurate than those based on the shape functions previously derived by Pan and Amadei (1996a).

For the SIF calculation, we employ the extrapolation method of the RCDs, which requires the analytical expression of the crack-tip displacements in terms of the SIFs. We assume, for simplicity, that there is a plane of material symmetry normal to the x_3-axis (or x_3-axis is a two-fold symmetry axis). Thus, there is no coupling of displacement u_3 with the components u_1 and u_2. For this case, the relation of the RCDs at a distance r behind the crack-tip and the SIFs can be found as (Sih et al., 1965; Sollero and Aliabadi, 1993; Pan and Amadei, 1996a)

$$\begin{aligned}
\Delta u_1 &= 2\sqrt{\frac{2r}{\pi}}(H_{11}K_{\mathrm{I}}+H_{12}K_{\mathrm{II}}),\\
\Delta u_2 &= 2\sqrt{\frac{2r}{\pi}}(H_{21}K_{\mathrm{I}}+H_{22}K_{\mathrm{II}}),\\
\Delta u_3 &= 2\sqrt{\frac{2r}{\pi}}\,\mathrm{Im}\left(\frac{-1}{c_{45}+\mu_3 c_{44}}\right)K_{\mathrm{III}},
\end{aligned} \tag{7}$$

where H_{ij} are coefficients depending on the material properties (Pan and Amadei, 1996a). Im denotes the imaginary part of a complex variable or function; c_{44} and c_{45} are the elements of the elastic stiffness matrix; and μ_3 is the third root of (9) below.

On the crack-tip element, equating the RCDs from the numerical calculation (5) to the analytical expression (7), one then obtains a set of algebraic equations from which the SIFs $K_{\mathrm{I}}, K_{\mathrm{II}}$ and K_{III} can be solved.

On the discretization of the boundary integral equations (3) and (4), it is noted that the Green's displacements and stresses (and their derivatives) and the particular solutions of displacements and stresses (tractions) need to be provided. This is discussed in the next two sections.

3. Green's functions in anisotropic full- and half-planes

The complex variable function method has been found to be very suitable for the study of 2-D anisotropic elastic media (Lekhnitskii, 1963). The Green's functions for point sources in such an infinite medium have been studied by several authors, notably by Lekhnitskii (1963), Eshelby et al. (1953) and Stroh (1958). For an anisotropic half-plane, the Green's functions

were studied by Suo (1990) using the one-complex-variable approach, and by Ting and co-workers (Ting, 1992; Ting and Barnett, 1991; Wei and Ting, 1994) based on the Stroh tensor method. We here follow the one-complex-varaible approach introduced by Suo (1990).

With three complex analytical functions $f_j(z_i)$, one can, in general, express displacements and stresses as (Lekhnitskii, 1963; Suo, 1990; Pan and Amadei, 1995)

$$\begin{aligned} u_i &= 2\,\mathrm{Re}\left[\sum_{j=1}^{3} A_{ij} f_j(z_j)\right], \\ \sigma_{2i} &= 2\,\mathrm{Re}\left[\sum_{j=1}^{3} L_{ij} f_j'(z_j)\right], \\ \sigma_{1i} &= -2\,\mathrm{Re}\left[\sum_{j=1}^{3} L_{ij}\mu_j f_j'(z_j)\right]. \end{aligned} \tag{8}$$

In these equations, $z_j = x + \mu_j y$. Re denotes the real part of a complex variable or function; and $\mu_j (j = 1, 2, 3)$ are three distinct complex roots with positive imaginary part of the following equation

$$l_4(\mu) l_2(\mu) - l_3^2(\mu) = 0, \tag{9}$$

where the complex functions l_2, l_3, and l_4 are given in Lekhnitskii (1963). Also in (8), the elements of the complex matrices $[\mathbf{L}]$ and $[\mathbf{A}]$ are functions of the compliance tensor a_{ij} and their expressions can be found in Lekhnitskii (1963), Suo (1990), or Pan and Amadei (1996a).

For a concentrated force acting at a source point (x^0, y^0), the complex functions in (8) can be expressed as (Suo, 1990)

$$f_j(z_j) = \sum_{k=1}^{3} \frac{-1}{2\pi} D_{jk} P_k \ln(z_j - z_j^0), \tag{10}$$

where $z_j^0 = x^0 + \mu_j y^0$; $P_k (k = 1, 2, 3)$ is the magnitude of the point force in the k-direction; and

$$\begin{aligned} \mathbf{D} &= \mathbf{A}^{-1}(\mathbf{B}^{-1} + \overline{\mathbf{B}}^{-1})^{-1}, \\ \mathbf{B} &= i\mathbf{A}\mathbf{L}^{-1}, \end{aligned} \tag{11}$$

where $i = \sqrt{-1}$, the overbar indicates complex conjugation and superscript -1 indicates matrix inversion.

For a half-plane problem, we let the medium occupy the lower half-plane $(y \leqslant 0)$ and $y = 0$ correspond to the traction-free flat surface. The Green's functions corresponding to the half-plane domain can be derived using the one-complex-variable approach (Suo, 1990; Pan et al., 1997). For displacements, these Green's functions are

$$U_{kl}^* = \frac{-1}{\pi}\,\mathrm{Re}\left\{\sum_{j=1}^{3} A_{1j}\left[D_{jk}\,1\mathrm{n}(z_j - z_j^0) - \sum_{i=1}^{3} E_{ji}\overline{D}_{ik}\,1\mathrm{n}(z_j - \overline{z}_i^0)\right]\right\}, \tag{12}$$

with

$$\mathbf{E} = \mathbf{L}^{-1}\overline{\mathbf{L}} \tag{13}$$

and for tractions, they are

$$T^*_{kl} = \frac{1}{\pi}\,\mathrm{Re}\left\{\sum_{j=1}^{3} L_{1j}\left[\frac{\mu_j n_x - n_y}{z_j - z_j^0}D_{jk} - \sum_{i=1}^{3} E_{ji}\frac{\mu_j n_x - n_y}{z_j - \overline{z}_i^0}\overline{D}_{ik}\right]\right\}, \tag{14}$$

with n_x and n_y being the outward normal components at the field point (x, y). In (12) and (14), the indices k and 1 take on the range of 1–3.

It is worthy to mention that the Green's functions in (12) and (14) can be used to solve both in-plane (plane stress and strain) and anti-plane problems in anisotropic half- or full-planes (for the full-plane case, the Green's functions are those given by the first summation terms in (12) and (14) (Pan and Amadei, 1996a)). Although the isotropic solution cannot be analytically reduced from the Green's functions (12) and (14), one can approximate it numerically by selecting a very weak anisotropic (or nearly isotropic) medium (Sollero et al., 1994; Pan and Amadei, 1996a).

4. Particular solutions of gravity

As we mentioned in Section 2, it the particular solutions corresponding to the body force of gravity can be derived in an exact closed-form, the single-domain BEM formulation presented in this paper can then be applied to solve the body force problem. For the gravity force, the exact closed-form solutions can be obtained in a similar way as for the corresponding half-space case (Amadei and Pan, 1992). These solutions were derived most recently by Pan et al. (1997), and we present here only the final results of the displacements and stresses.

Assuming that the gravity has components g_x and g_y, respectively, in the x- and y-directions, the particular solutions of dispalcements can be found as (Pan et al., 1997)

$$\begin{aligned} u_x^p &= a_1\rho g_x x^2 + b_1\rho g_y y^2, \\ u_y^p &= a_2\rho g_x x^2 + b_2\rho g_y y^2, \\ u_z^p &= 0, \end{aligned} \tag{15}$$

where coefficients a_i and b_i depend on the elastic stiffness and their expressions are given in the Appendix A of Pan et al. (1997).

Similarly, the particular stresses can be expressed as (Pan et al., 1997)

$$\begin{bmatrix} \sigma_{11}^p \\ \sigma_{22}^p \\ \sigma_{23}^p \\ \sigma_{13}^p \\ \sigma_{12}^p \end{bmatrix} = \begin{bmatrix} d_{11} & d_{12} \\ d_{21} & d_{22} \\ d_{41} & d_{42} \\ d_{51} & d_{52} \\ d_{61} & d_{62} \end{bmatrix} \begin{bmatrix} \rho g_x x \\ \rho g_y y \end{bmatrix}. \tag{16}$$

Again, d_{ij} depend on the elastic coefficients and their expressions are given in the Appendix A of Pan et al. (1997).

Table 1. SIFs for a circular-arc crack in an infinite domain.

	Numer.			Exact (Tada et al., 1985)		
α	$K_{\rm I}/\sigma\sqrt{\pi a}$	$K_{\rm II}/\sigma\sqrt{\pi a}$	$K_{\rm III}/\tau\sqrt{\pi a}$	$K_{\rm I}/\sigma\sqrt{\pi a}$	$K_{\rm II}/\sigma\sqrt{\pi a}$	$K_{\rm III}/\tau\sqrt{\pi a}$
30°	0.5547	0.3299	0.6873	0.5501	0.3304	0.6830
45°	0.4662	0.5145	0.7879	0.4574	0.5112	0.7769

5. Numerical examples

The aforementioned Green's functions and the particular solutions have been incorporated into the boundary integral equations presented in Section 2, and the results have been programmed. In this section, a number of benchmark examples are selected to verify the program and to show the efficiency, accuracy and versatility of the present BEM formulation for problems related to the calculation of the SIFs in anisotropic media. For the isotropic case, the Young's modulus was assumed as $E = 40$(GPa) and the Poisson's ratio as $v = 0.25$; For the anisotropic case, the elastic constants will be specified in the particular example. A plane stress condition will be assumed unless otherwise specified. Whenever possible, we have also included the SIF $K_{\rm III}$ for the future reference.

EXAMPLE 1. A curved crack in an infinite domain.

Shown in Figure 2 is a circular-arc crack under a far-field tensile stress σ and anti-plane shear stress τ. The arc is located symmetrically with respect to the y-axis and has a radius a. The half angle of the arc is α. We used only 20 discontinuous quadratic elements to discretize the curved crack surface. The numerically calculated SIFs for $\alpha = 30^\circ$ and 45°, as well as the exact closed-form solutions (Tada et al., 1985), are listed in Table 1. As can be observed from Table 1 that the numerical results are in good agreement with the exact closed form solutions.

EXAMPLE 2. Multiple or branched cracks in an infinite domain.

Figure 3 shows a scheme of two cracks under a far-field tensile stress σ and anti-plane shear stress τ. While the first crack is horizontal, the second one is inclined 60° to the horizontal direction. Both cracks have the same length $2a$ and their centers are separated at a distance d such that the ratio $2a/d = 0.9$. We used only 10 discontinuous quadratic elements for each crack surface. The results for the normalized SIFs at the crack-tips A, B, C and D are given in Table 2. This problem was solved previously by Chen (1995) using a singular integral equation method. As shown in Table 2 that the present numerical results are in excellent agreement with those obtained by chen (1995).

Shown in Figure 4 is a branched crack under a far-field tensile stress σ and anti-plane shear stress τ. The main crack has a length a and each branch has a length b, with ratios $b/a = 0.6$ and 0.05. The branches are located symmetrically on both sides of the main crack and inclined at $\alpha = 45^\circ$ to it. It is noteworthy that at the junction of the branch cracks, the RCD and the integration of the traction should satisfy, respectively, the continuity and equilibrium conditions derived by Ammons and Vable (1996). However, collocations at the branch point can be avoided using discontinuous elements. Here, we used 10 discontinuous quadratic elements for the main crack surface, 6 elements for each branch when $b/a = 0.6$,

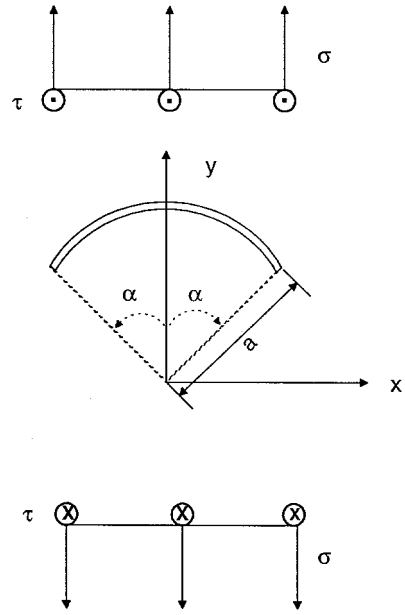

Figure 2. A curved (circular-arc) crack under a far-field tensile stress σ and anti-plane shear stress τ.

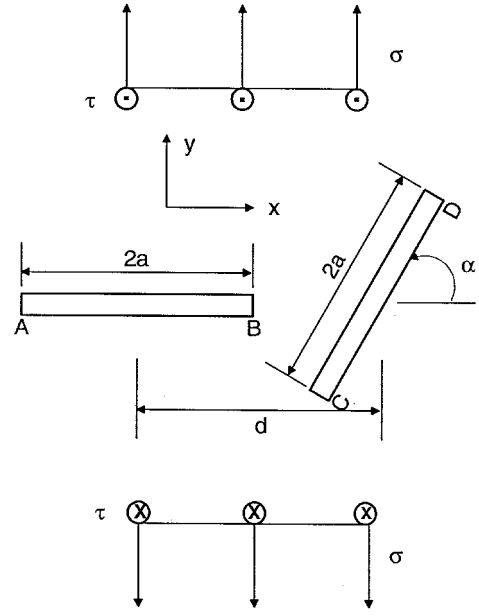

Figure 3. Two cracks under a far-field tensile stress σ and anti-plane shear stress τ.

and only 1 element for each branch when $b/a = 0.05$. The numerical results for this problem were documented in Murakami (1987) and were also solved recently by Ammons and Vable (1996) using their single-domain BEM formulation. In Table 3, the SIFs at the crack-tips A and B are given for the two ratios of b/a and compared to those obtained by Ammons and Vable (1996) and documented in Murakami (1987).

Table 2. SIFs for two cracks in an infinite domain.

	$K_{\mathrm{I}}^{A}/\sigma\sqrt{\pi a}$	$K_{\mathrm{II}}^{A}/\sigma\sqrt{\pi a}$	$K_{\mathrm{III}}^{A}/\tau\sqrt{\pi a}$	$K_{\mathrm{I}}^{B}/\sigma\sqrt{\pi a}$	$K_{\mathrm{II}}^{B}/\sigma\sqrt{\pi a}$	$K_{\mathrm{III}}^{B}/\tau\sqrt{\pi a}$
Present	1.0312	−0.0300	1.0160	1.0757	−0.0395	1.0269
Chen (1995)	1.0311	−0.0300	—	1.0757	−0.0394	—
	$K_{\mathrm{I}}^{C}/\sigma\sqrt{\pi a}$	$K_{\mathrm{II}}^{C}/\sigma\sqrt{\pi a}$	$K_{\mathrm{III}}^{C}/\tau\sqrt{\pi a}$	$K_{\mathrm{I}}^{D}/\sigma\sqrt{\pi a}$	$K_{\mathrm{II}}^{D}/\sigma\sqrt{\pi a}$	$K_{\mathrm{III}}^{D}/\tau\sqrt{\pi a}$
Present	0.3109	0.5149	0.4830	0.3089	0.4525	0.5580
Chen (1995)	0.3101	0.5149	—	0.3086	0.4525	—

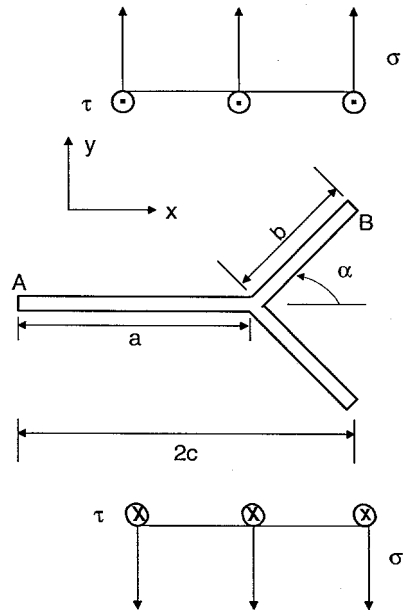

Figure 4. A branched crack under a far-field tensile stress σ and anti-plane shear stress τ.

Table 3. SIFs for a branched crack in an infinite domain.

		$K_{\mathrm{I}}^{A}/\sigma\sqrt{\pi c}$	$K_{\mathrm{III}}^{A}/\tau\sqrt{\pi c}$	$K_{\mathrm{I}}^{B}/\sigma\sqrt{\pi c}$	$K_{\mathrm{II}}^{B}/\sigma\sqrt{\pi c}$	$K_{\mathrm{III}}^{B}/\tau\sqrt{\pi c}$
$b/a = 0.6$	Present	1.0299	1.1137	0.4974	0.4846	0.7194
	Murakami, (1987)	1.029	—	0.497	0.485	—
	Ammons and Vable, (1996)	1.027	—	0.496	0.484	—
$b/a = 0.05$	Present	1.0056	1.0140	0.5862	0.2989	0.7852
	Murakami, (1987)	1.006	—	0.593	0.297	—
	Ammons and Vable, (1996)	1.004	—	0.593	0.297	—

EXAMPLE 3. Cracks in a half-plane.

Figure 5 shows an internal vertical crack in a half-plane under a far-field tensile stress σ and anti-plane shear stress τ. The crack length is $2a$ and its center is at a distance d from the traction-free flat surface such that the ratio $a/d = 0.5$. Twenty discontinuous quadratic elements were used to discretize the crack surface. This problem was solved by Noda and Matsuo (1993) using a singular integral equation method with continuously distributed dislocations. The SIFs at the crack tips A and B are given in Table 4 which shows clearly that our numerical results are very close to those obtained by Noda and Matsuo (1993).

Figure 6 shows an internal horizontal crack in a half-plane under a uniform pressure p and anti-plane shear q along the crack surface. The crack length is 2a and the distance of the crack to the traction-free flat surface is h. Again, we used 20 discontinuous quadratic elements to discretize the crack surface. Itou (1994) solved the problem using an integral equation method combined with the Fourier transform. In Table 5, the SIFs are given for various ratios of h/a and compared to those obtained by Itou's (1994).

EXAMPLE 4. Edge cracks in a finite domain.

Figure 7 shows an edge crack in a rectangular plate which is subjected to a uniaxial tension σ. The geometry of the problem is such that $h/w = a/w = 0.5$. This problem was solved before by Civelek and Erdogan (1982), and recently by Portela et al. (1992), using their DBEM with the J-integral method. Here we used 25 quadratic elements for the no-crack boundary and 5 discontinuous quadratic elements for the crack surface. Our result and those obtained by Civelek and Erdogan (1982) and Portela et al. (1992) are listed in Table 6, which indicates that these results are very close to each other.

Shown in Figure 8 is a scheme of double edge cracks emanating from a hole in a rectangular plate which is subjected to a uniaxial tension σ. The geometry of the problem is such that $2h/w = a/r = 1$ and $2(r + a) = w/2$. We used 32 quadratic elements for the no-crack boundary and 5 discontinuous quadratic elements for each crack. Chang and Mear (1995) solved the problem by forming a single-domain BEM formulation in which the tangential derivatives of the RCDs, instead of the RCDs themselves, were used as unknowns. Our normalized SIF and that determined by Chang and Mear (1995) are given in Table 7 which again shows excellent agreement between these two SIFs.

EXAMPLE 5. An inclined crack in an anisotropic and finite domain.

Figure 9 shows an anisotropic and finite rectangular plate with a central crack inclined 45° to the horizontal direction under a uniaxial tension σ in the y-direction. The ratios of crack length to width, and of height to width are $a/w = 0.2$ and $h/w = 2$, respectively. The material is of glass-epoxy with the elastic properties $E_1 = 48.26\,\text{GPa}$, $E_2 = 17.24\,\text{GPa}$, $v_{12} = 0.29$ and $G_{12} = 6.89\,\text{GPa}$ (Gandhi, 1972). The direction of the fibers was rotated from $\psi = 0°$ to $\psi = 180°$. This problem was solved by Gandhi (1972) using a modified mapping collocation technique, by Sollero and Aliabadi (1995a) using the DBEM formulation, and recently by Pan and Amadei (1996a) using the single-domain BEM formulation which is similar to the one presented in this paper. In both (Pan and Amadei, 1996a) and (Sollero and Aliabadi, 1995a), the J- integral method was used to evaluate the SIFs. Here, as in Pan and Amadei (1996a), we used 10 discontinuous quadratic elements on the crack surface and 32 quadratic elements on the no-crack boundary. But instead of using the J- integral, we used directly the crack

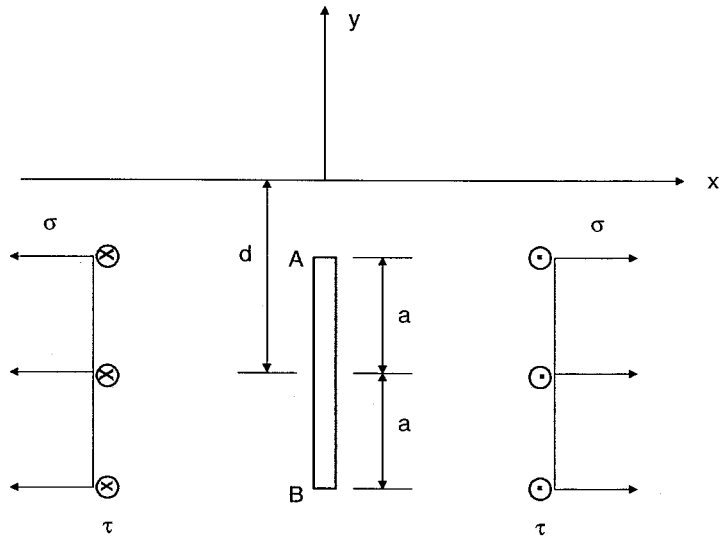

Figure 5. An internal vertical crack in half-plane under a far-field tensile stress σ and anti-plane shear stress τ.

Table 4. SIFs for a vertical crack in a half-plane under a far-field stress.

	$K_{\mathrm{I}}^{A}/\sigma\sqrt{\pi a}$	$K_{\mathrm{III}}^{A}/\tau\sqrt{\pi a}$	$K_{\mathrm{I}}^{B}/\sigma\sqrt{\pi a}$	$K_{\mathrm{III}}^{B}/\tau\sqrt{\pi a}$
Present	1.0920	1.0487	1.0546	1.0287
Noda and Matsuo (1993)	1.0913	—	1.0539	—

Table 5. SIFs for a horizontal crack in half-plane under pressure.

	Itou (1994)		Present		
h/a	$K_{\mathrm{I}}/p\sqrt{\pi a}$	$K_{\mathrm{II}}/p\sqrt{\pi a}$	$K_{\mathrm{I}}/p\sqrt{\pi a}$	$K_{\mathrm{II}}/p\sqrt{\pi a}$	$K_{\mathrm{III}}/q\sqrt{\pi a}$
2.0	1.1634	0.0367	1.1643	0.0367	1.0291
1.0	1.5110	0.1849	1.5130	0.1849	1.0922
0.4	2.9051	0.9939	2.9176	0.9962	1.3025

Table 6. SIF $K_{\mathrm{I}}/\sigma\sqrt{\pi a}$ of an edge crack in a finite domain (Figure 7).

Present	Civelek and Erdogan (1982)	Portela et al. (1992)
2.992	3.010	3.021

Table 7. SIF $K_{\mathrm{I}}/\sigma\sqrt{\pi(r+a)}$ of an edge crack in a finite domain (Figure 8).

Present	Chang and Mear (1995)
1.5636	1.5627

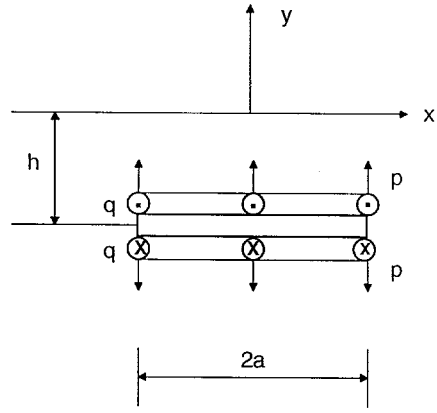

Figure 6. An internal horizontal crack in a half-plane under a uniform pressure p and anti-plane shear stress q along the crack surface.

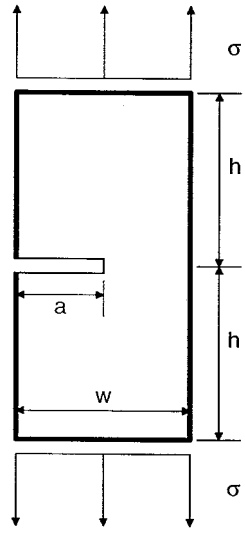

Figure 7. An edge crack in a rectangular plate which is subjected to a uniaxial tension σ.

displacement relations (5–7). The normalized SIFs for this mixed mode problem are given in Tables 8 and 9. As indicated by Tables 8 and 9 that the SIFs calculated by the present method are closest to the accurate results obtained by Gandhi (1972).

EXAMPLE 6. A crack in a finite domain under an anti-plane loading.

An off-center crack in a finite plate subjected to a uniform anti-plane shear τ is shown in Figure 10. The geometry is such that $a/w = a/h = 0.5$. We used 10 discontinuous quadratic elements for the crack surface and 20 quadratic elements for the no-crack boundary. For $e/w = 0.5$, the normalized SIF $K_{\rm III}/\tau\sqrt{\pi a}$ obtained with the current BEM formulation is 1.154, which is close to 1.178 obtained by Ma and Zhang (1991) using an integral equation method. For $e/w = 0$, i.e., the central crack case, the SIF obtained with the present method is given in the second row of Table 10 and compared to those in Liu and Altiero (1992) and Ma (1988). As can be observed from Table 10 that these results are very close to each other.

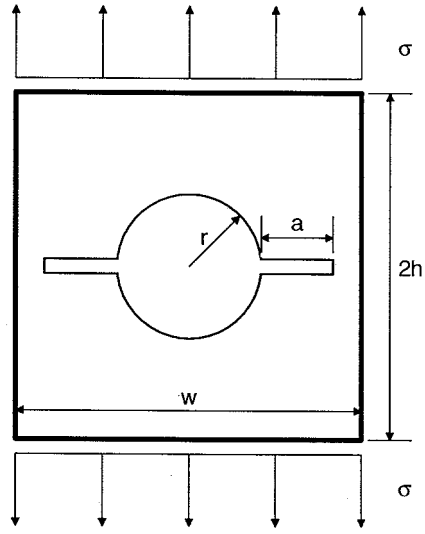

Figure 8. Double edge cracks emanating from a hole in a rectangular plate which is subjected to a uniaxial tension σ.

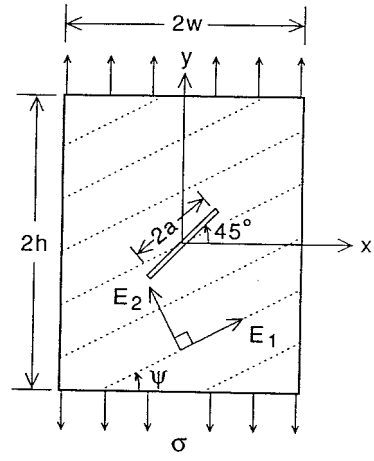

Figure 9. An anisotropic and finite rectangular plate with a central crack inclined 45° to the horizontal direction under a uniaxial tension σ.

Table 8. SIF $K_I/\sigma\sqrt{\pi a}$ for an internal crack in a finite domain.

ψ	Sollero and Aliabadi (1995a)	Pan and Amadei (1996a)	Gandhi (1972)	Present
0°	0.517	0.519	0.522	0.5228
45°	0.513	0.516	0.515	0.5153
90°	0.515	0.537	0.513	0.5133
105°	0.518	0.507	0.517	0.5165
120°	0.526	0.520	0.524	0.5240
135°	0.535	0.532	0.532	0.5316
180°	0.517	0.519	0.522	0.5228

Table 9. SIF $K_{\rm II}/\sigma\sqrt{\pi a}$ for an internal crack in a finite domain.

ψ	Sollero and Aliabadi (1995a)	Pan and Amadei (1996a)	Gandhi (1972)	Present
0°	0.506	0.504	0.507	0.5076
45°	0.502	0.505	0.505	0.5048
90°	0.510	0.532	0.509	0.5090
105°	0.512	0.502	0.510	0.5107
120°	0.513	0.508	0.512	0.5117
135°	0.514	0.511	0.511	0.5111
180°	0.506	0.504	0.507	0.5076

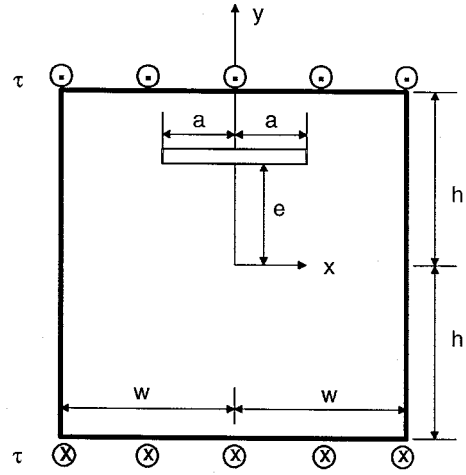

Figure 10. An off-center crack in a finite plate subjected to a uniform anti-plane shear stress τ.

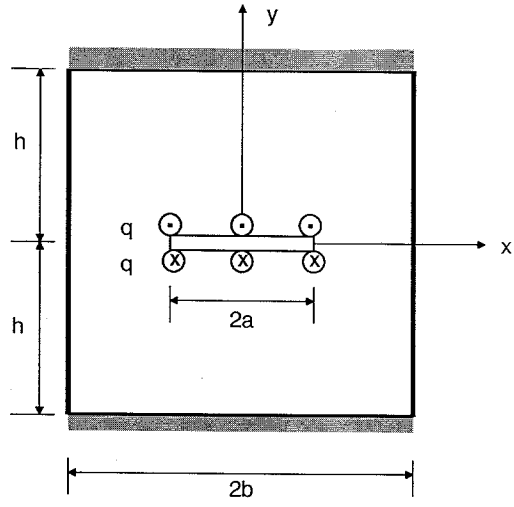

Figure 11. A central crack in a finite plate with fixed edges parallel to the crack. The crack surface is subjected to a uniform anti-plane shear stress q.

Table 10. SIFs for the anti-plane case.

	Present	Ma (1988; 1989)	Liu and Altiero (1992)
$K_{\mathrm{III}}/\tau\sqrt{\pi a}$	1.1276	1.130	1.127
$K_{\mathrm{III}}/q\sqrt{\pi a}$	0.9231	0.923	0.920

Table 11. SIF $K_{\mathrm{I}}/(h/w)^2\rho g w\sqrt{\pi a}$ for the body force case.

	Present	Leung and Su (1995)
Fixed	0.4813	0.48
Simple	4.0430	4.42

Figure 11 shows a central crack in a finite plate with fixed edges parallel to the crack. The geometry is such that $a/b = a/h = 0.5$. The crack surface is subjected to a uniform anti-plane shear q. In the third row of Table 10, the SIF obtained with the present BEM formulation is given and compared to those in Liu and Altiero (1992) and Ma (1989).

EXAMPLE 7. A crack under the body force of gravity.

Figure 12 shows an edge crack in a finite domain subjected to the body force of gravity g with fixed end support in (a) and simple support in (b). The geometry of the problem is such that $h/w = 4$ and $a/w = 0.5$. A plane strain condition was assumed for this example. We used 10 discontinuous quadratic elements for the crack surface and 48 quadratic elements for the no-crack boundary. The normalized SIFs are given in Table 11 and are compared to those obtained by Leung and Su (1995) using the finite element method.

6. Conclusions

The single-domain BEM formulation proposed recently by Pan and Amadei (1996a) has been extended in this paper to the general fracture mechanics analysis in cracked 2-D anisotropic

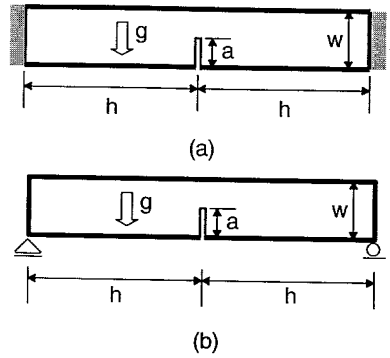

Figure 12. An edge crack in a finite domain subjected to the body force of gravity g, with fixed end support in (a) and simple support in (b).

elastic media. Instead of using the J-integral for the calculation of the SIFs, the author proposed the extrapolation method of the relative crack displacement combined with a new set of crack-tip shape functions. As such, the body force, pressurized crack, and curved crack cases can all be easily studied in a unified and versatile way. Extensions have also been made for the anti-plane and half-plane cases.

Numerical examples of the calculation of the SIFs for various benchmark problems were conducted and excellent agreement with previously published results was obtained.

Since the present method is simple, efficient, accurate and versatile, the author believes that the single-domain BEM formulation presented in this paper could be a powerful numerical tool which can find applications to various fracture mechanics problems in 2-D anisotropic media. Some of the related problems are currently under investigation by the author and results will be submitted in a separate paper.

Acknowledgment

The author would like to thank both reviewers for their constructive comments which lead to improvements on the earlier version of the manuscript. The work presented in this paper was supported by National Science Foundation under Grant CMS-9622645.

References

Aliabadi, M.H. (1997). Boundary element formulations in fracture mechanics. *Applied Mechanics Review* **50**, 83–96.

Amadei, B. and Pan, E. (1992). Gravitational stresses in anisotropic rock masses with inclined strata. *International Journal of Rock Mechanics and Mining Science & Geomechanics Abstracts* **29**, 225–236.

Ammons, B.A. and Vable, M. (1996). Boundary element analysis of cracks. *International Journal of Solids and Structures* **33**, 1853–1865.

Blandford, G.E., Ingraffea, A.R. and Liggett, J.A. (1981). Two-dimensional stress intensity factor computations using the boundary element method. *International Journal for Numerical Methods in Engineering* **17**, 387–404.

Chang, C. and Mear, M.E. (1995). A boundary element method for two dimensional linear elastic fracture analysis. *International Journal of Fracture* **74**, 219–251.

Chen, Y.Z. (1995). Hypersingular integral equation approach for the multiple crack problem in an infinite plate. *Acta Mechanica* **108**, 121–131.

Civelek, M.B. and Erdogan, F. (1982). Crack problems for a rectangular sheet and an infinite strip. *International Journal of Fracture* **19**, 139–159.

Crouch, S.L. and Starfield, A.M. (1983). *Boundary Element Methods in Solid Mechanics*, George Allen and Unwin Publishers, London.

Dumir, P.C. and Mehta, A.K. (1987). Boundary element solution for elastic orthotropic half-plane problems. *Computers and Structures* **26**, 431–438.

Eshelby, J.D., Read, W.T. and Shockley, W. (1953). Anisotropic elasticity with applications to dislocations theory. *Acta Metallurgica* **1**, 251–259.

Gandhi, K.R. (1972). Analysis of an inclined crack centrally placed in an orthotropic rectangular plate. *Journal of Strain Analysis* **7**, 157–162.

Gray, L.J., Martha, L.F. and Ingraffea, A.R. (1990). Hypersingular integrals in boundary element fracture analysis. *International Journal for Numerical Methods in Engineering* **29**, 1135–1158.

Hong, H.K. and Chen, J.T. (1988). Derivations of integral equations of elasticity. *Journal of Engineering Mechanics* **114**, 1028–1044.

Itou, S. (1994). Stress intensity factors around a crack parallel to a free surface of a half-plane. *International Journal of Fracture* **67**, 179–185.

Lee, J.S. (1995). Boundary element method for electroelastic interaction in piezoceramics. *Engineering Analysis with Boundary Elements* **15**, 321–328.

Lekhnitskii, S.G. (1963). *Theory of Elasticity of an Anisotropic Body*, Holden Day, San Francisco.

Leung, A.Y.T. and Su, R.K.L. (1995). Body-force linear elastic stress intensity factor calculation using fractal two level finite element method. *Engineering Fracture Mechanics* **51**, 879–888.

Liu, N. and Altiero, N.J. (1991). Multiple cracks and branch cracks in finite plane bodies. *Mechanics Research Communications* **18**, 233–244.

Liu, N. and Altiero, N.J. (1992). An integral equation method applied to mode III crack problems. *Engineering Fracture Mechanics* **41**, 587–596.

Liu, N., Altiero, N.J. and Sur, U. (1990). An alternative integral equation approach applied to kinked cracks in finite plane bodies. *Computer Methods in Applied Mechanics and Engineering* **84**, 211–226.

Ma, S.W. (1988). A central crack in a rectangular sheet where its boundary is subjected to an arbitrary anti-plane load. *Engineering Fracture Mechanics* **30**, 435–443.

Ma, S.W. (1989). A central crack of mode III in a rectangular sheet with fixed edges. *International Journal of Fracture* **39**, 323–329.

Ma, S.W. and Zhang, L.X. (1991). A new solution of an eccentric crack off the center line of a rectangular sheet for mode-III. *Engineering Fracture Mechanics* **40**, 1–7.

Murakami, Y. (1987). *Stress Intensity Factors Handbook*, Pergamon Press, Oxford.

Noda, N.A. and Matsuo, T. (1993). Numerical solutions of singular integral equations having Cauchy-type singular kernel by means of expansion method. *International Journal of Fracture* **63**, 229–245.

Pan, E. and Amadei, B. (1995). Stress concentration at irregular surfaces of anisotropic half-spaces. *Acta Mechanica* **113**, 119–135.

Pan, E. and Amadei, B. (1996a). Fracture mechanics analysis of cracked 2-D anisotropic media with a new formulation of the boundary element method. *International Journal of Fracture* **77**, 161–174.

Pan, E. and Amadei, B. (1996b). A 3-D boundary element formulation of anisotropic elasticity with gravity. *Applied Mathematical Modelling* **20**, 114–120.

Pan, E., Chen, C.S. and Amadei, B. (1997). A BEM formulation for anisotropic half-plane problems. *Engineering Analysis with Boundary Elements* **20**, 185–195.

Portela, A., Aliabadi, M.H. and Rooke, D.P. (1992). The dual boundary element method: Effective implementation for crack problems. *International Journal for Numerical Methods in Engineering* **33**, 1269–1287.

Sih, G.C., Paris, P.C. and Irwin, G.R. (1965). On cracks in rectilinearly anisotropic bodies. *International Journal of Fracture* **3**, 189–203.

Snyder, M.D. and Cruse, T.A. (1975). Boundary-integral analysis of anisotropic cracked plates. *International Journal of Fracture* **11**, 315–328.

Sollero, P. and Aliabadi, M.H. (1993). Fracture mechanics analysis of anisotropic composite laminates by the boundary element method. *International Journal of Fracture* **64**, 269–284.

Sollero, P. and Aliabadi, M.H. (1995a). Anisotropic analysis of cracks in composite laminates using the dual boundary element method. *Composite structures* **31**, 229–233.

Sollero, P. and Aliabadi, M.H. (1995b). Dual boundary element analysis of anisotropic crack problems. In *Boundary Elements XVII*, C. A. Brebbia et al. (eds.) Computational Mechanics Publications, Southampton, 267–278.

Sollero, P., Aliabadi, M.H. and Rooke, D.P. (1994). Anisotropic analysis of cracks emanating from circular holes in composite laminates using the boundary element method. *Engineering Fracture Mechanics* **49**, 213–224.

Stroh, A.N. (1958). Dislocations and cracks in anisotropic elasticity. *The Philosophical Magazine* **7**, 625– 646.

Suo, Z. (1990). Singularities, interfaces and cracks in dissimilar anisotropic media. *Proceedings of the Royal Society* (London), A**427**, 331–358.

Sur, U. and Altiero, N.J. (1988). An alternative integral equation approach for curved and kinked cracks. *International Journal of Fracture* **38**, 25–41.

Tada, H., Paris, P.C. and Irwin, G.R. (1985). *The Stress Analysis of Cracks Handbook*, 2nd Edition, Paris Productions Incorporated, Missouri.

Telles, J.C.F. and Brebbia, C.A. (1981). Boundary element solution for half-plane problems. *International Journal of Solids and Structures* **17**, 1149–1158.

Ting, T.C.T. (1992). Image singularities of Green's functions for anisotropic elastic half-spaces and bimaterials. *Quarterly Journal of Mechanics and Applied Mathematics* **45**, 119–139.

Ting, T.C.T. and Barnett, D.M. (1993). Image force on line dislocations in anisotropic elastic half-spaces with a fixed boundary. *International Journal of Solids and Structures* **30**, 313–323.

Tsamasphyros, G. and Dimou, G. (1990). Gauss quadrature rules for finite part integrals. *International Journal for Numerical Methods in Engineering* **30**, 13–26.

Wei, L. and Ting, T.C.T. (1994). Explicit expressions of the Barnett-Lothe tensors for anisotropic materials. *Journal of Elasticity* **36**, 67–83.